Mon. Not. R. Astron. Soc. **352,** 249–257 (2004) doi:10.1111/j.1365-2966.2004.07918.x

The formation of a helium white dwarf in a close binary system with diffusion

O. G. Benvenuto[1,2★†] and M. A. De Vito[1★‡]

[1]*Facultad de Ciencias Astronómicas y Geofísicas, Universidad Nacional de La Plata, Paseo del Bosque S/N, (1900) La Plata, Argentina*
[2]*Departamento de Astronomía y Astrofísica, Pontificia Universidad Católica, Vicuña Mackenna 4860, Casilla 306, Santiago, Chile*

Accepted 2004 April 8. Received 2004 April 7; in original form 2003 December 30

ABSTRACT

We study the evolution of a system composed of a 1.4-$M_\odot$ neutron star and a normal, solar composition star of 2 $M_\odot$ in orbit with a period of 1 d. Calculations were performed employing the binary HYDRO code presented by Benvenuto & De Vito that handle the mass transfer rate in a fully implicit way. We then included the main standard physical ingredients together with the diffusion processes and a proper outer boundary condition. We have assumed fully non-conservative mass transfer episodes.

In order to study the interplay of mass loss episodes and diffusion we considered evolutionary sequences with and without diffusion in which all Roche lobe overflows (RLOFs) produce mass transfer. Another two sequences in which thermonuclearly driven RLOFs were not allowed to drive mass transfer have been computed with and without diffusion. As far as we are aware, this study represents the first binary evolution calculations in which diffusion is considered.

The system produces a helium white dwarf of ∼0.21 $M_\odot$ in an orbit with a period of ∼4.3 d for the four cases. We find that mass transfer episodes induced by hydrogen thermonuclear flashes drive a tiny amount of mass transfer. As diffusion produces stronger flashes, the amount of hydrogen-rich matter transferred is slightly higher than in the models without diffusion.

We find that diffusion is the main agent in determining the evolutionary time-scale of low-mass white dwarfs even in the presence of mass transfer episodes.

Key words: binaries: general – stars: evolution – stars: interiors.

1 INTRODUCTION

At present, it is a well established fact that low-mass white dwarf (WD) stars should be formed during the evolution of close binary systems (CBSs). These objects are expected to have a helium-rich interior simply because they have a mass below the threshold for helium ignition of approximately 0.45 $M_\odot$. If they were formed as consequence of single star evolution, we would have to wait for time-scales far in excess of the present age of the Universe to find some of them.

The formation of helium WDs in CBSs was first investigated long ago by Kippenhahn, Kohl & Weigert (1967) and Kippenhahn, Thomas & Weigert (1968). They found that these objects are formed during the evolution of low-mass CBSs and that the cooling evolution is suddenly stopped by thermonuclear flashes that are able to expand the star to produce further Roche lobe overflows (RLOFs).

Since sometime ago, low-mass WDs have been discovered as companions to millisecond pulsars (MSP). This fact sparked interest in helium WDs in order to investigate the deep physical links between both members of a given pair. In particular, it represents an attractive possibility to infer characteristics of the neutron star behaving as an MSP by studying the WD in detail. Studies devoted to helium WD properties are those of Alberts et al. (1996); Althaus & Benvenuto (1997); Benvenuto & Althaus (1998); Driebe et al. (1998, 1999); Hansen & Phinney (1998a); Althaus & Benvenuto (2000); Schönberner, Driebe & Blöcker (2000); Althaus, Serenelli & Benvenuto (2001a,b,c); Serenelli et al. (2001, 2002) and Rohrmann et al. (2002). Sarna, Ergma & Gerškevitš-Antipova (2000) considered the problem in the frame of detailed binary evolution calculations. More recently, Podsiadlowski, Rappaport & Pfahl (2002) have also computed the evolution of some CBS configurations that give rise to the formation of helium WDs. Also, Nelson & Rappaport (2003) have explored in detail the evolutionary scenarios of binary systems with initial periods shorter than the bifurcation one leading to the formation of ultracompact binaries with periods shorter than an hour. In contrast, in this paper we shall deal with a system with an initial period larger than the bifurcation one leading to wider binaries.

★E-mail: obenvenuto@fcaglp.unlp.edu.ar; (OGB); adevito@fcaglp.unlp.edu.ar (MADV)
†Member of the Carrera del Investigador Científico, Comisión de Investigaciones Científicas de la Provincia de Buenos Aires (CIC), Argentina.
‡Fellow of the CIC.

Remarkably, the first WD found as companion of an MSP in globular clusters was detected by Edmonds et al. (2001). Among recent observations of low-mass WD companion to MSPs we should quote those by van Kerkwijk et al. (2000) who have detected the WD companion of the binary MSP PSR B1855+09, the mass of which is known accurately from measurements of the Shapiro delay of the pulsar signal, $M_{\rm WD} = 0.258^{+0.028}_{-0.016}$ $M_\odot$. The orbital period of this binary MSP is 12.3 d. More recently, Bassa, van Kerkwijk & Kulkarni (2003a) found a faint bluish counterpart for the binary MSP PSR J02018+4232. The spectra confirm that the companion is a helium WD and, in spite of the fact that observations are of insufficient quality to put a strong constraint on the surface gravity, the best fit indicates a low $\log g$ value and hence low mass ($\approx$0.2 $M_\odot$). On the other hand, independently, Ferraro et al. (2003) and Bassa et al. (2003a) have identified the optical binary companion to the MSP PSR J1911-5958A, located in the halo of the galactic globular cluster NGC 6752. This object turned out to be a blue star where its position in the colour–magnitude diagram is consistent with the cooling sequence of a low-mass ($\approx$0.17–0.20 $M_\odot$), low-metallicity helium WD at the cluster distance. This is the second helium WD with a mass in this range that has been found to orbit an MSP in a galactic globular cluster. Also, Sigurdsson et al. (2003) have detected two companions for the pulsar B 1620-26, one of stellar mass and one of planetary mass. The colour and magnitude of the stellar companion indicate a WD of 0.34 ± 0.04 $M_\odot$ of age 4.8×10^8 yr. For previous detections of this kind of objects we refer the reader to the paper by Hansen & Phinney (1998b).

From a theoretical point of view, it was soon realized that the key ingredient of WD models is the hydrogen mass fraction in the star. Consequently, this called for a detailed treatment of the outer layers of the star. Iben & MacDonald (1985) demonstrated the relevance of diffusion in the evolution of intermediate mass CO WDs, while Iben & Tutukov (1986) found it to also be important in low-mass WDs.

More recently, Althaus et al. (2001a,b,c) revisited the problem of the formation of helium WDs. In doing so, they mimicked binary evolution by abstracting mass to a 1-$M_\odot$ object on the red giant branch (RGB). The main goal of these papers was to investigate in detail the role of diffusion during the evolution as a pre-WD object. They allowed gravitational settling, chemical and thermal diffusion to operate. However, they did not considered the possibility of any mass transfer episode after detachment from the RGB. Perhaps the main result of Althaus et al. (2001a,b,c) was finding that for models with diffusion there exists a threshold mass value $M_{\rm th}$ above which the object undergoes several thermonuclear flashes in which a large fraction of the hydrogen present in the star is burnt out. Consequently, as the star enters on the final cooling track it evolves rapidly, reaching very low luminosities on a time-scale comparable with the age of the Universe. In contrast, in models without diffusion, evolutionary time-scales are much longer, making it difficult to reconcile with observations. For WDs belonging to CBSs in companion with MSP, WD ages should be comparable to the characteristic age of pulsars $\tau_{\rm PSR} = P/2\dot{P}$ (for a pulsar of period P with period derivative $\dot{P}$ that had an initial period P_0 such that $P_0 \ll P$ and braking index $n = 3$). This should be so, because it is generally accepted that the MSP is recycled by accretion from its normal companion. However, it was found that the WD was much dimmer than predicted by models without diffusion, which should be interpreted as a consequence of a faster evolution. This was the case of the companion of PSR B1855+09.

For objects with masses below $M_{\rm th}$ no thermonuclear flash occurs and the star does not suffer from another RLOF. Consequently, it retains a thick hydrogen layer, able to support nuclear burning, forcing the WD to remain bright for a very long time. This is the case of the companion of PSR J1012+5307.

It is our aim in the the present paper to revisit the problem of the formation and the evolution of helium WDs in CBSs by performing full binary computations considering diffusion starting with models on the main sequence all the way down to the stages of evolution of the remnant as a very cool WD. As far as we are aware this is the first time such a study has been carried out. In this way we largely generalize the previous studies from our group on this topic. In doing so, we preferred to concentrate on a particular binary system, deferring a detailed exploration of the huge parameter space (masses, orbital periods, chemical compositions, etc.) to future publications. To be specific, we have chosen to study a CBS composed of a 2-$M_\odot$ normal star together with a neutron star with a 'canonical' mass of 1.4 $M_\odot$ on an initial orbit with a period of 1 d. We assumed solar chemical composition with $Z = 0.02$ for which $M_{\rm th} \approx 0.19$ $M_\odot$ (Althaus et al. 2001b).

In order to explore the role and interplay of mass loss episodes and diffusion we have constructed four complete evolutionary calculations:

(i) case A: diffusion, all RLOF operate (including flash-induced RLOF);
(ii) case B: diffusion, without flash-induced RLOF;
(iii) case C: no diffusion, all RLOF operate;
(iv) case D: no diffusion, without flash-induced RLOF.

Regarding mass transfer episodes we have chosen to study the case of fully non-conservative conditions, i.e. those in which all the matter transferred from the primary star is lost from the system carrying away all its intrinsic angular momentum. We do so in order to obtain the strongest possible RLOFs which, in turn, will produce the largest mass transfer episodes. In this sense, we shall find an upper limit to the effects of RLOFs on the whole evolution of the star, in particular regarding the ages of very cool WDs.

The reminder of the paper is organized as follows. In Section 2 we describe our code paying special attention to the changes we implemented in the scheme for computing mass transfer episodes. Then, in Section 3 we describe the evolutionary results for the four cases considered here. Finally, in Section 4 we discuss the implications of our calculations and summarize the main conclusions of this work.

2 NUMERICAL METHODS

In the computations presented below we have employed the code for computing stellar evolution in close binary systems presented in Benvenuto & De Vito (2003). Now we have incorporated the full physical ingredients with the aim of getting state-of-the-art evolutionary results. In particular, we have included a complete set of nuclear reactions to describe hydrogen and helium burning together with diffusion processes. For more details on the considered physics, see, e.g., Althaus et al. (2001a).

Regarding the outer boundary condition, we have incorporated the formula given by Ritter (1988) for computing the mass transfer rate (MTR) $\dot{M}$:

$$\dot{M} = -\dot{M}_0 \exp\left(-\frac{R_{\rm L} - R}{H_{\rm P}}\right), \qquad (1)$$

where $\dot{M}_0$ is the MTR for a star that exactly fills the Roche lobe (see Ritter's paper for its definition), $R_{\rm L}$ is the equivalent radius of

the Roche lobe (see below), R is the stellar radius and H_P is the photospheric pressure scaleheight. We have considered that a mass transfer episode is underway when $R \geqslant R_L - \xi H_P$ with $\xi = 16$. In this way the star begins (ends) to transfer mass in a very natural and smooth way. This has been completely adequate for the purpose of carrying out the calculations presented below.

3 EVOLUTIONARY CALCULATIONS

In order to present the numerical calculations we shall describe in detail the sequence for which all physical ingredients were considered (case A) in which we allowed diffusion and mass transfer in each RLOF to operate. The evolutionary track in the Hertzsprung–Russell (HR) diagram corresponding to case A is shown in Fig. 1. The 2-$M_\odot$ object begins to evolve and the first RLOF occurs (point 1 in Table 1) when it is still burning hydrogen in the centre. Thus, we are dealing with Class A mass transfer, as defined by Kippenhahn & Weigert (1967). At that moment the hydrogen central abundance is $X_H = 0.214\,578$. From there on, as consequence of the orbital evolution of the binary, the primary star undergoes a huge mass loss (see the first panel of Fig. 2), which continues up to the moment (point 2 in Table 1) at which central hydrogen exhaustion occurs. The star contracts and mass transfer is stopped; at that moment the mass of the primary is of 1.592 52 $M_\odot$. Little later, as consequence of the formation of a shell hydrogen burning zone, the star inflates and mass transfer starts again (point 3), and stands on a long period at which the star loses almost 90 per cent of the initial mass, ending with a mass of 0.220 07 $M_\odot$. Hereafter we shall consider these two RLOF episodes as an initial RLOF in order to differentiate it from the other flash-induced RLOFs. During the initial mass transfer episode, the hydrogen content of the outermost layers decreased to a minimum value of $\approx$0.3 because mass transfer dredges up layers that were previously undergoing appreciable nuclear burning (see Fig. 3). This increase in the mean molecular weight of the plasma present in the outer layers of the star favours the contraction of the primary star. At point 4 the star detaches from the Roche lobe, and from then on the star evolves bluewards very rapidly up to approximately the moment at which reaches a local maximum in the effective temperature. After such maximum effective temperature, evolution appreciably slows down allowing diffusion to have enough time to evolve the hydrogen profile. Here, hydrogen tends to float simply because it is the lighter element present in the plasma.

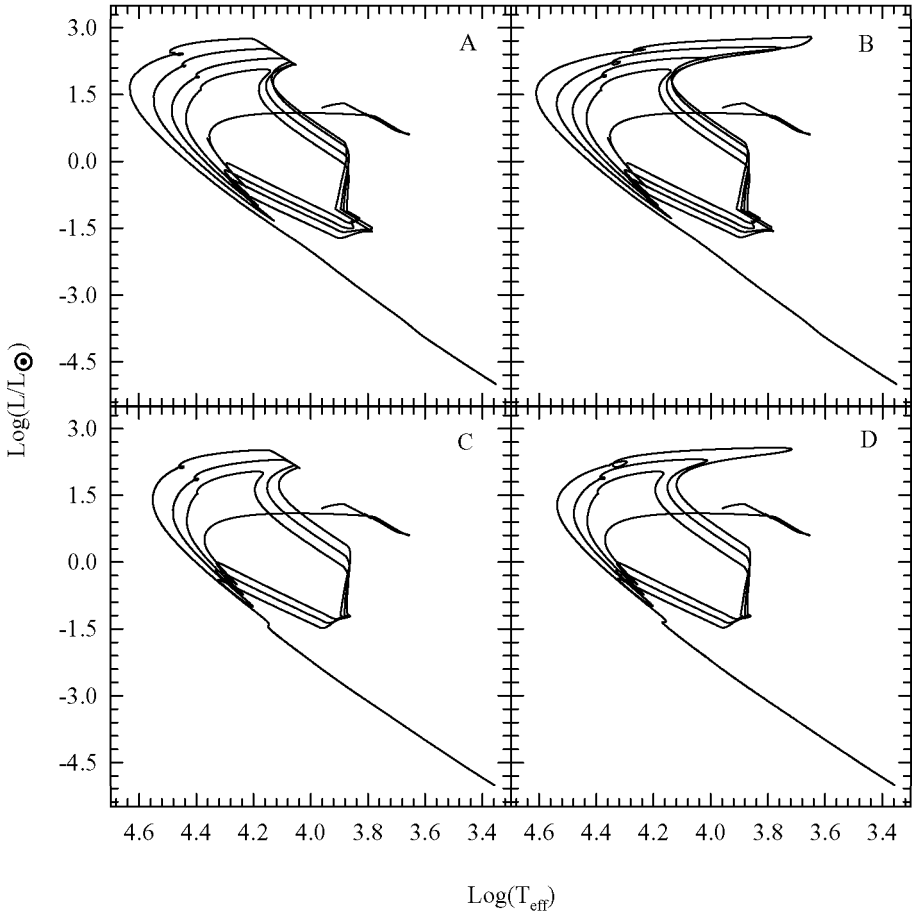

Figure 1. The evolutionary tracks for the primary component of the binary system initially composed of a normal main-sequence, solar composition star of $M = 2.0\ M_\odot$ together with a neutron star of 1.4 $M_\odot$, with a period of $P = 1.0$ d for the four cases considered in this paper. Each panel is labelled as in the main text: A, diffusion, all RLOFs operate; B, diffusion, no flash-induced RLOF operates; C, no diffusion, all RLOFs operate; D, no diffusion, no flash-induced RLOF operates. Note that models with diffusion suffer from four hydrogen thermonuclear flashes, while models without diffusion undergo only three. This is independent of considering or ignoring the flash-induced mass transfer episodes. Here, for the sake of clarity we decided not to indicate the points given in Tables 1–3.

Table 1. Selected stages of the evolution of a system composed of a 1.4-$M_\odot$ neutron star and a normal, solar composition star of 2 $M_\odot$ in orbit with an initial period of 1 d. Here we have considered diffusion and mass transfer during each RLOF episode (case A). Points labelled with odd (even) numbers correspond to the beginning (end) of a mass transfer episode in Fig. 1. The last point corresponds to the end of the computation.

Point	$\log(L/L_\odot)$	$\log(L_{nuc}/L_\odot)$	$\log(T_{eff})$	X_s	Age (Myr)	$M_*/M_\odot$	P (d)	M_H/M_*
0	1.291 596	1.291 596	3.999 353	0.700 000	0.000 000	2.000 00	1.000	0.700 000
1	1.306 425	1.325 886	3.883 615	0.719 213	675.907 133	2.000 00	0.990	0.631 826
2	1.069 236	1.085 928	3.808 278	0.700 722	898.696 085	1.592 52	1.273	0.593 744
3	1.052 254	1.083 202	3.803 819	0.700 938	899.305 975	1.592 52	1.273	0.593 691
4	1.007 000	0.998 083	3.774 765	0.297 839	1057.346 100	0.220 07	4.309	0.029 015
5	2.158 183	1.557 922	4.071 799	0.213 738	1126.419 320	0.220 07	4.309	0.005 668
6	2.310 374	1.558 437	4.115 358	0.213 738	1126.419 557	0.219 90	4.310	0.005 490
7	2.151 000	1.900 315	4.068 010	0.172 838	1149.826 078	0.219 90	4.310	0.004 322
8	2.521 391	1.900 161	4.170 841	0.172 838	1149.826 261	0.219 19	4.313	0.003 738
9	2.210 319	2.297 033	4.080 971	0.119 486	1214.483 908	0.219 19	4.313	0.002 783
10	2.754 083	2.360 036	4.233 749	0.119 486	1214.484 019	0.218 01	4.320	0.002 141
11	−5.001 480	$-\infty$	3.352 189	0.998 488	18 995.499 104	0.218 01	4.316	0.001 609

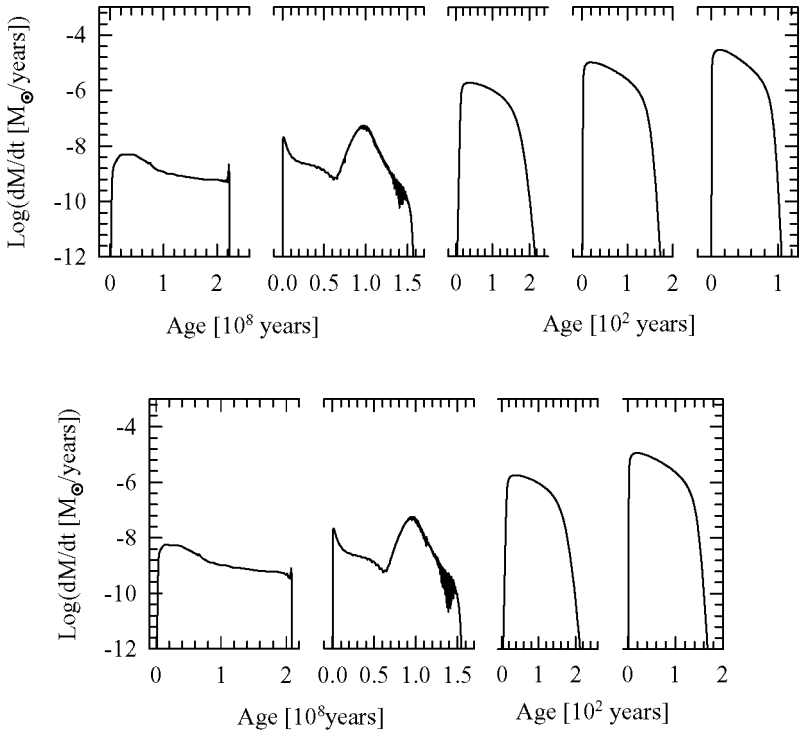

Figure 2. The mass transfer rates from the primary star corresponding to the evolutionary tracks shown in Fig. 1 in which mass transfer is considered at each RLOF. The upper panel corresponds to case A (with diffusion), while the lower panel depicts the results for case C (without diffusion). From left to right panels correspond to each RLOF episode. For clarity, in each panel we have counted time from the beginning of each mass transfer episode. For the absolute value of time we simply have to add the time of the onset of RLOF given in Tables 1 and 3, respectively. Note that, in both cases, the initial RLOF is very prolonged. The first happens when the star is still burning hydrogen at its core. At core exhaustion mass transfer ends, and when the star expands due to the outwards motion of the hydrogen shell burning, a new RLOF occurs. We called these two RLOFs the initial RLOF. In the lower and upper panels these events are almost the same due to the fact that the effects of diffusion are barely noticeable at these early stages. The subsequent episodes are due to thermonuclear flashes. Note that their duration is six orders of magnitude shorter.

This is clearly shown as a steep increase in Fig. 3 where we show the surface hydrogen abundance[1] of the model as a function of time.

In contrast with the behaviour of surface abundance, at the bottom of the hydrogen envelope, hydrogen tend to sink now as a consequence of the large abundance gradients. The net effect is that, while the outer layers become richer in hydrogen, diffusion is fuelling hot layers. Then, when the hydrogen rich layers become degenerate and conduction eases the energy flux outwards, hydrogen becomes hot enough to ignite. Now, in degenerate conditions, ignition is unstable (see Fig. 4). Consequently, evolution suddenly accelerates and a hydrogen thermonuclear flash occurs. Such a flash is not strong

[1] As a matter of facts this is the abundance of the first point of the discrete mesh of the model, located at $\log 1 - M_r/M \approx -8$.

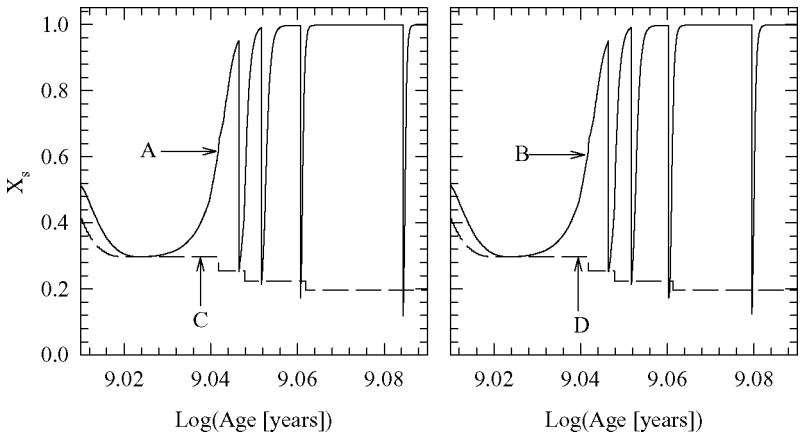

Figure 3. The hydrogen abundance in the outermost layers of the primary star. Here we considered the hydrogen abundance at the first point in the grid corresponding to $1 - M_r/M \approx 10^{-8}$. In the left-hand panel we depict the results for the models in which RLOFs are allowed, whereas the right-hand panel depicts the case for the models in which mass transfer driven by thermonuclearly induced RLOFs is neglected. Each curve is labelled as in Fig. 1. Note the enormous differences in the behaviour of the outer layers in the cases with and without diffusion. However, abundances are barely affected by the allowance of mass transfer, as is clearly noticeable in view of the similarities of the plots in each panel. In the sequences corresponding to case A, due to mixing, mass transferred during each RLOF has a chemical composition corresponding to a minimum in hydrogen abundance. Such a composition is very similar to that of the plasma transferred in the models of case C without diffusion. See the main text for further details.

enough to inflate the star to force a new RLOF. Regarding surface abundances, we should note that little time after the thermonuclear flash occurs, the star develops a deep outer convective zone covering very hydrogen rich layers up to others in which hydrogen is almost a trace. As a consequence, hydrogen abundance suddenly drops[2] down to a value similar to the one the star had at the end of the initial RLOF (see Fig. 3 and Table 1). The referred mixing is noticeable in the evolutionary track (Fig. 1) as a sudden change of slope after the minimum in the effective temperature and luminosity of the star. After mixing, the outer layers of the star continue expanding to become near to producing a RLOF, but begin to contract before this happens. After maximum radius is reached, the star undergoes a rapid contraction up to its maximum effective temperature, and once again time-scales become long enough for diffusion to operate. The star again floats hydrogen at outer layers and fuels others that will make the star undergo a second thermonuclear flash. Now the star has a higher degree of degeneracy in the critical layers, making the flash stronger than the previous one. From there on the star undergoes much the same evolution as in the previous flash, but now the star inflates enough to undergo a third RLOF event. The conditions at the onset of this third RLOF correspond to point 5 in Table 1.

Obviously, this third RLOF is very different from the initial one. Now the envelope is very dilute and so, a tiny amount of stellar mass occupies a large portion of its radius. Consequently, very little mass is transferred from the primary in contrast to the initial RLOF in which the primary transferred approximately 90 per cent of it initial mass. The MTR during this third RLOF is depicted in the third panel of Fig. 2. Remarkably, the mass lost from the primary star during this third RLOF has a low hydrogen abundance due to the previous mixing.

After few thousands of years transferring mass, the star contracts again repeating essentially the same evolution the star followed after the first thermonuclear flash. Remarkably, the star has lost hydrogen, due to nuclear burning and to mass transfer (see Fig. 5). However, the star still has an amount of hydrogen high enough to force the star to undergo another flash. Now the flash is rather more violent than the previous one producing another RLOF.

In order to gain clarity, we have chosen to discuss in detail the loop due to the last thermonuclear flash. In Fig. 6 we show the excursion of the star in the HR diagram indicating the main physical agents acting in the star together with some particular models (solid dots). The hydrogen profiles corresponding to models before and just at the end of (after) the RLOF are shown in Fig. 7 (Fig. 8). Some relevant characteristics of these models are presented in Table 2.

The hydrogen profile for some of the models is indicated in Fig. 7 corresponding to stages prior to and just after the last RLOF. Up to model labelled 11 000 (the model number in the sequence) the outwards motion of the profile is due to the nuclear burning during the flash. After model 11 000 on (not shown in the figure) the profile moves outwards as a consequence of the mass transfer episode, which ends in model 11 200. Note that the loss of hydrogen is somewhat tiny (points 9 and 10 in Table 1).

In Fig. 8 the curve labelled as 14 500 corresponds to stages somewhat after RLOF. Curves labelled as 15 000–15 050 are displaced outwards due to nuclear burning, while curve 15 075 corresponds to a profile modified by diffusion. Note that the tail of the hydrogen profile becomes appreciably deeper approximately when the outermost layers become saturated by hydrogen.

From our calculations we find that after only four hydrogen thermonuclear flashes the star is able to enter on the final cooling track of a helium WD (see Fig. 4). The evolutionary time-scale of the model is presented in Fig. 9. Note that the nuclear energy released at such advanced stages of evolution is a minor contribution to the total energy balance of the star. As a consequence the star obtains heat from its relic thermal content, which forces a rapid evolution, reaching very low luminosities in time-scales comparable to the age of the Universe. We stopped the calculation when the object reached $\log L/L_\odot = -5$, at that moment the star had an age of approximately 19 Gyr.

Now, let us discuss the results corresponding to case C in which we allowed all the RLOF to drive the mass transfer, but we have neglected diffusion (see Table 3). The evolutionary track for this

[2] Note that this is consequence of the fact that we have assumed instantaneous mixing throughout convective zones.

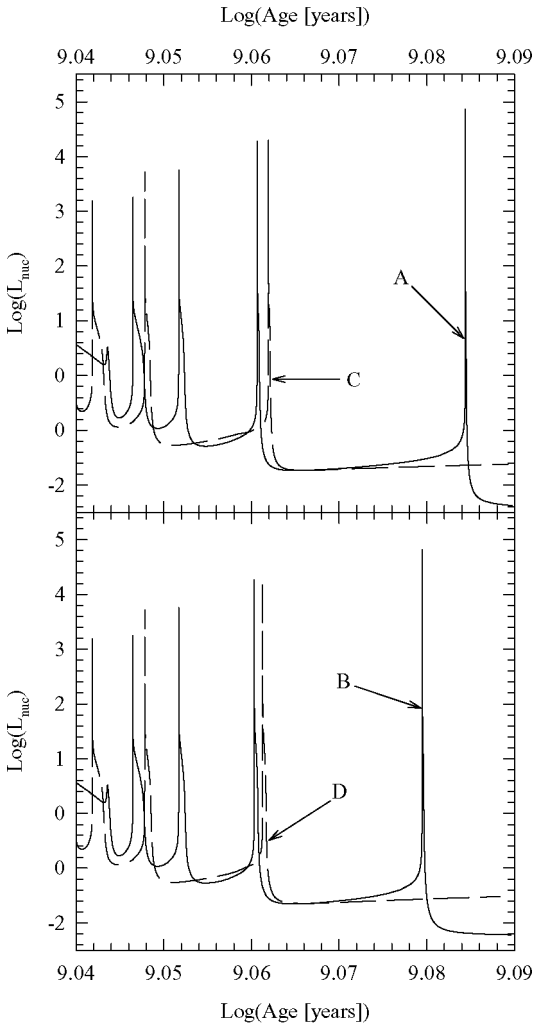

Figure 4. The logarithm of the nuclear luminosity (in solar units) versus the age relationship for the four evolutionary sequences studied in this paper. Labels A–D refer to the evolutionary tracks A–D in Fig. 1. Note that models with (without) diffusion undergo four (three) thermonuclear flashes.

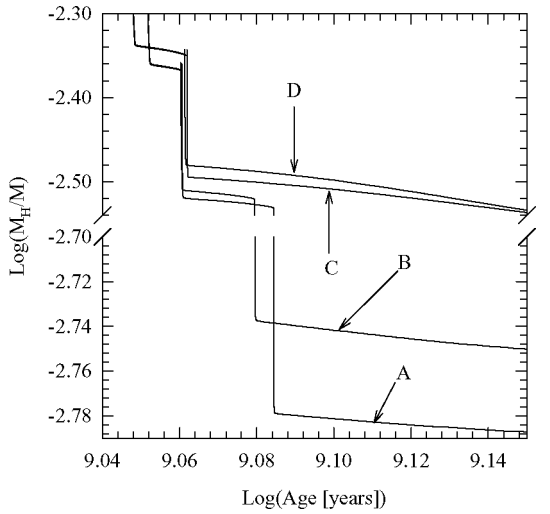

Figure 5. The logarithm of the hydrogen mass fraction present in the star versus time for the four cases of evolution presented in this paper during the last thermonuclear flashes. Labels A–D refer to the evolutionary tracks A–D in Fig. 1. Note that after thermonuclear flashes, models with diffusion have a lower hydrogen fraction. Also, as may be expected, the hydrogen mass fraction is lower for models in which RLOFs operate at these stages. Models without diffusion end their flash episodes with a higher hydrogen content, which is subsequently burnt out during the final cooling track. Note the change in the vertical scale of this figure above and below the break in the vertical axis. See the main text for further details.

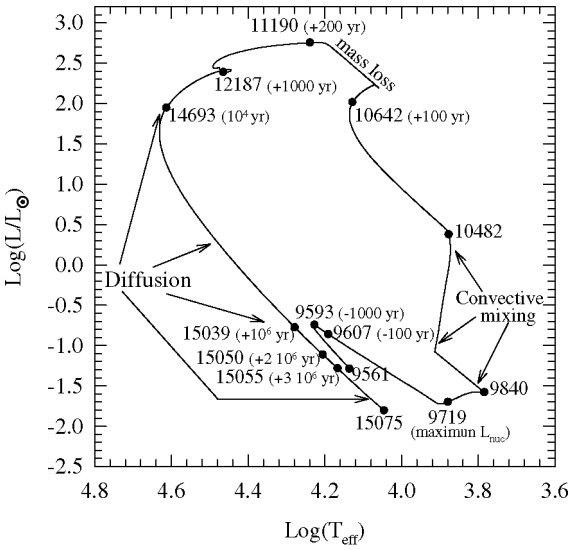

Figure 6. The last loop in the HR diagram corresponding to case A evolution. Solid dots correspond to selected stages, for some of which the hydrogen profiles are presented below and are labelled with the number of the model in the computed sequence. Ages are counted with respect to the maximum in the nuclear energy release. We also note the most important physical effects in each portion of the track. Note the sudden changes in the shape of the track due to convective mixing and mass loss.

case is shown in Fig. 1, panel C. Here, the evolution prior to the end of the initial RLOF is very similar to that corresponding to case A. In other words, diffusion has a negligible effect on these evolutionary stages. Perhaps, the main difference is the increase in hydrogen surface abundances prior to the initial RLOF found in case A is absent here (see Table 1). However, differences in the evolution are quite significant after the end of initial RLOF.

As here, by assumption, the physical agents able to modify abundances are only nuclear reactions and convection, obviously, the outermost layers of the hydrogen-rich layers are not enriched by hydrogen and simultaneously no fuelling occurs at the bottom. Consequently, the evolution is very different. Notably, the star undergoes only three thermonuclear flashes and outer layers have rather constant abundances in spite of the fact that they also develop outer convection zones after each flash. As in the previous case we computed the evolution up to when the object reached $\log L/L_{\odot} = -5$ with an age of approximately 25.65 Gyr. Thus, evolution is markedly slower than in case A. This is due to the fact that here thermonuclear flashes are weaker, burning less hydrogen. As a consequence, the star is able to undergo appreciable thermonuclear energy release during the final cooling track as a helium WD. In this regard, note that nuclear burning remains the dominant energy source of the star up to ages of 10 Gyr (see Fig. 9).

The sequence of models corresponding to case B (case C) is very similar to that corresponding to case A (case D) and will not be

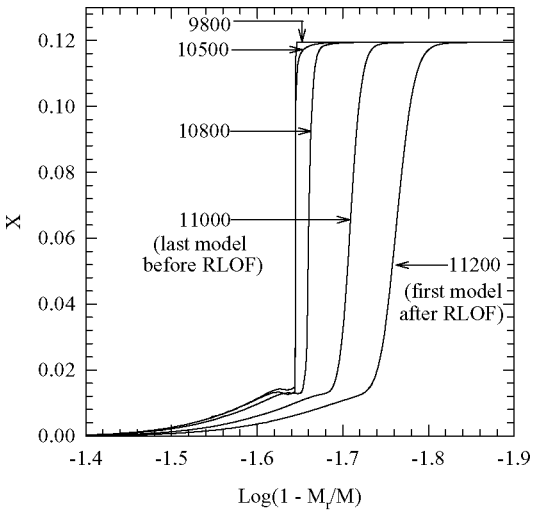

Figure 7. The hydrogen profile for some of the models indicated in Fig. 6 corresponding to stages prior to and just after the last RLOF. Up to the model labelled 11 000 the outwards motion of the profile is due to nuclear burning. From this model to that labelled 11 200 the motion is almost entirely due to the mass transfer during the RLOF.

discussed in detail. The obvious major difference is related to the size the star is able to reach just after the thermonuclear flashes. As in case B (case D) it is assumed that there is no limit imposed by the size of the Roche lobe, after thermonuclear flashes, the star reaches effective temperatures far lower than those allowed in the case of the occurrence of RLOFs. Quite noticeably, the evolutionary time-scale of the final WD cooling track is largely independent of the occurrence of any thermonuclearly flash-induced RLOF (see Fig. 9).

Another interesting difference arises regarding the characteristic time-scale of the evolution of the models from the red part of the diagram to the maximum effective temperature conditions. We have found that in such stages, the evolution of models for which thermonuclearly induced RLOFs are allowed suffer from a much faster evolution regardless of the allowance or not of diffusion.

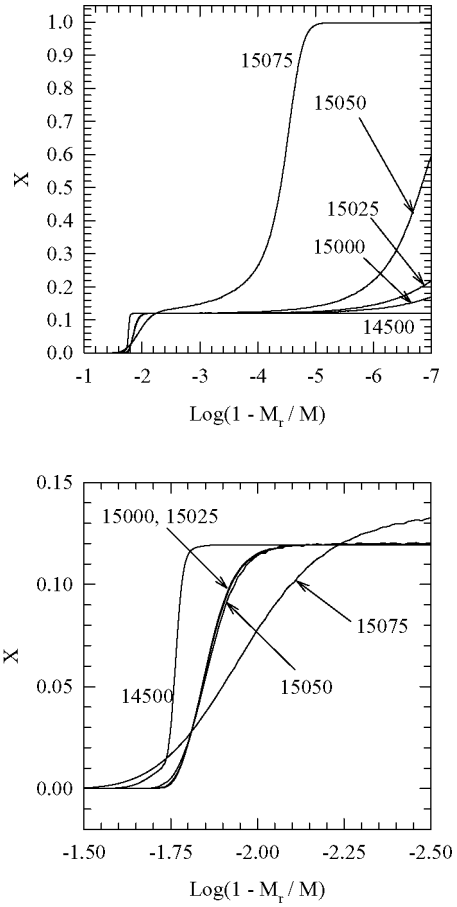

Figure 8. The hydrogen profile for some of the models indicated in Fig. 6 corresponding to stages after the last RLOF. The upper panel represents the whole hydrogen profile, while the lower one highlights the bottom of the profile. The evolution of the outer parts of the profile are fully dominated by diffusion. In the bottom there is an interplay between nuclear burning and diffusion. Initially nuclear reactions dominate (models 14 500–15 050), but at later times (model 15 075) chemical diffusion drives a large amount of hydrogen inwards.

Table 2. Selected stages of the evolution of the primary star of the system corresponding to case A. We have selected relevant models in a loop shown at Fig. 6. Model denotes for the number of models in the evolutionary calculation.

Model	$\log(L/L_\odot)$	$\log(L_{nuc}/L_\odot)$	$\log(T_{eff})$	X_s	Age (Myr)	M_H/M_*
9561	−1.285 417	−1.464 898	4.136 383	0.997 875	1206.136 861	0.002 962
9593	−0.743 989	1.319 834	4.227 583	0.997 875	1214.482 831	0.002 921
9607	−0.859 529	2.616 561	4.191 011	0.997 875	1214.483 706	0.002 915
9719	−1.700 589	4.860 120	3.878 964	0.997 875	1214.483 802	0.002 820
9840	−1.577 785	4.118 219	3.784 233	0.997 875	1214.483 809	0.002 790
10 482	0.378 350	2.338 424	3.877 158	0.119 486	1214.483 895	0.002 783
10 642	2.014 473	2.313 509	4.127 957	0.119 486	1214.483 902	0.002 783
10 714	2.210 319	2.297 033	4.080 971	0.119 486	1214.483 908	0.002 783
11 190	2.754 083	2.360 036	4.233 749	0.119 486	1214.484 019	0.002 141
12 187	2.390 152	2.739 479	4.464 822	0.119 486	1214.484 802	0.002 120
14 693	1.948 789	1.939 478	4.613 450	0.120 118	1214.493 795	0.002 062
15 039	−0.774 868	−1.657 584	4.278 570	0.395 631	1215.485 203	0.001 664
15 050	−1.112 451	−2.015 089	4.205 475	0.720 579	1216.420 781	0.001 664
15 055	−1.281 705	−2.151 893	4.167 198	0.921 884	1217.429 788	0.001 663
15 075	−1.805 696	−2.445 395	4.045 660	0.998 488	1267.968 504	0.001 653

Table 3. Selected stages of the evolution of a system composed of a 1.4-$M_\odot$ neutron star and a normal, solar composition star of 2 $M_\odot$ in orbit with a period of 1 d. Here mass transfer is allowed to occur during each RLOF episode, but diffusion has been neglected (case C). Points labelled with odd (even) numbers correspond to the beginning (end) of a mass transfer episode. The last point corresponds to the end of the computation.

Model	$\log(L/L_\odot)$	$\log(L_{nuc}/L_\odot)$	$\log(T_{eff})$	X_s	Age (Myr)	$M_*/M_\odot$	P (d)	M_H/M_*
0	1.291 596	1.291 596	3.999 353	0.700 000	0.000 000	2.000 00	1.000	0.700 000
1	1.305 931	1.325 651	3.883 688	0.700 000	683.258 119	2.000 00	0.990	0.631 100
2	1.080 234	1.081 842	3.811 255	0.699 873	892.518 745	1.601 19	1.266	0.595 018
3	1.059 051	1.092 015	3.805 732	0.699 873	893.302 911	1.601 19	1.266	0.594 950
4	1.011 273	0.998 631	3.776 142	0.297 567	1049.362 320	0.220 33	4.307	0.028 800
5	2.147 837	1.441 249	4.068 767	0.224 255	1116.384 319	0.220 33	4.307	0.005 821
6	2.297 723	1.446 788	4.111 879	0.224 255	1116.384 550	0.220 18	4.308	0.005 645
7	2.099 698	1.812 834	4.054 606	0.196 021	1153.232 534	0.220 18	4.308	0.004 501
8	2.520 010	1.808 553	4.171 450	0.196 021	1153.232 711	0.219 43	4.312	0.003 816
9	−5.011 041	$-\infty$	3.356 698	0.196 019	25 653.632 359	0.219 43	4.308	0.001 758

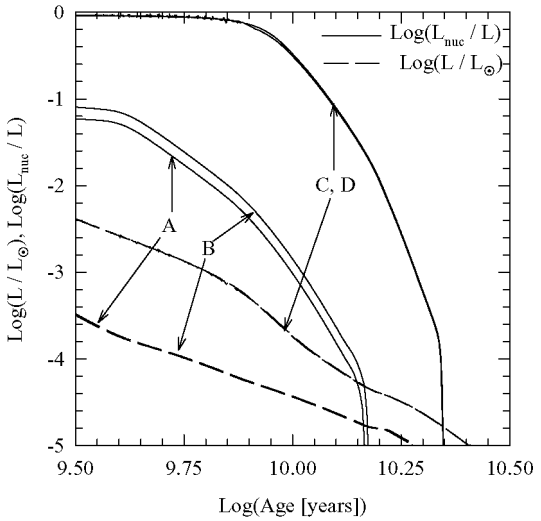

Figure 9. The logarithm of the photon luminosity and the nuclear luminosity fraction released during the last stages of the evolution of the models considered in this paper. Labels A–D refer to the evolutionary tracks A–D in Fig. 1. Models without diffusion have a much larger nuclear activity at advanced evolutionary stages, which slows down the evolution in an appreciable way. Remarkably, the ages of these objects are largely determined by the allowance of diffusion, whereas considering or neglecting thermonuclearly induced RLOFs has a negligible effect on stellar ages.

To be specific, from minimum to maximum effective temperature, case B models take $\approx 10^6$ yr, while models with RLOF spend only $\approx 10^4$ yr from Roche lobe detachment to maximum effective temperature. This, obviously indicates that it should be more difficult to find objects at such conditions than predicted in models without thermonuclearly-induced RLOFs. Also, note in Fig. 1 that the subflashes (little loops in the evolutionary tracks occurring when the star is evolving bluewards) happen at different effective temperatures depending on the allowance of RLOFs. In fact, in models with (without) RLOFs subflashes occur at higher (lower) effective temperatures for consecutive thermonuclear flashes. This is true irrespective of the allowance or not of diffusion.

4 DISCUSSION AND CONCLUSIONS

In this work we have computed the evolution of a binary system composed of a neutron star with a 'canonical mass' of 1.4 $M_\odot$ and a normal, population I main-sequence star of 2 $M_\odot$ in orbit with a 1-d period. We have performed the calculations employing an updated version of the code presented in Benvenuto & De Vito (2003) in which we have included the main standard physical ingredients together with diffusion processes. Also a proper outer boundary condition was incorporated following Ritter (1988), see Section 2.

In order to explore the role of mass transfer episodes from the primary star and its interplay with diffusion we have considered four situations: diffusion, all RLOF operate (case A); diffusion, no flash-induced RLOF operates (case B); no diffusion, all RLOF operate (case C); and no diffusion, no flash-induced RLOF operates (case D). See the introduction for further details.

As far as we are aware, these calculations represent the first detailed study of binary evolution considering diffusion. In this sense, this work represents a natural generalization of the results presented by Althaus et al. (2001a) in which the binary evolution processes were mimicked by forcing a 1-$M_\odot$ star on the red giant branch to undergo an appropriate mass-loss rate. Now the proper inclusion of the specific processes that govern binary evolution offer us a more physically sound description of the formation of low-mass, helium white dwarfs. In particular, now we have the possibility of connecting stellar structure and evolution with the orbital parameters of the systems allowing for a deeper comparison with observations.

From the results presented in the previous sections, it is clear that diffusion is far more important in determining the time-scale of the evolution of the stars than mass transfer episodes during flash-induced RLOFs. This is especially true when the object reaches the final cooling track. We found that time-scales are almost insensitive to the occurrence of flash-induced RLOF episodes (see Fig. 9). This constitutes the main result of the present work.

ACKNOWLEDGMENTS

We thank our referee, Professor Philipp Podsiadlowski for comments and suggestions that allowed to improve the clarity of the original version. OGB is supported by FONDAP Center for Astrophysics 15010003.

REFERENCES

Alberts F., Savonije G.J. van den Heuvel E.P.J., Pols O.R., 1996, Nat, 380, 676
Althaus L.G., Benvenuto O.G., 1997, ApJ, 477, 313
Althaus L.G., Benvenuto O.G., 2000, MNRAS, 317, 952
Althaus L.G., Serenelli A.M., Benvenuto O.G., 2001a, ApJ, 554, 1110

Althaus L.G., Serenelli A.M., Benvenuto O.G., 2001b, MNRAS, 324, 617
Althaus L.G., Serenelli A.M., Benvenuto O.G., 2001c, MNRAS, 323, 471
Bassa C.G., van Kerkwijk M.H., Kulkarni S.R., 2003a, A&A, 403, 1067
Bassa C.G., Verbunt F., van Kerkwijk M.H., Homer L., 2003b, A&A, 409, L31
Benvenuto O.G., Althaus L.G., 1998, MNRAS, 293, 177
Benvenuto O.G., De Vito M.A., 2003, MNRAS, 342, 50
Driebe T., Schoenberner D., Bloecker T., Herwig F., 1998, A&A, 339, 123
Driebe T., Blöcker T., Schönberner D., Herwig F., 1999, A&A, 350, 89
Edmonds P.D., Gilliland R.L., Heinke C.O., Grindlay J.E., Camilo F., 2001, ApJ, 557, L57
Ferraro F., Possenti A., Sabbi E., D'Amico N., 2003, ApJ, 596, L211
Hansen B.M.S., Phinney E.S., 1998a, MNRAS, 294, 557
Hansen B.M.S., Phinney E.S., 1998b, MNRAS, 294, 569
Iben I., MacDonald J., 1985, ApJ, 296, 540
Iben I.J., Tutukov A.V., 1986, ApJ, 311, 742
Kippenhahn R., Weigert A., 1967, Zap, 65, 251
Kippenhahn R., Kohl K., Weigert A., 1967, Zap, 66, 58
Kippenhahn R., Thomas H.-C., Weigert A., 1968, Zap, 69, 265
Nelson L.A., Rappaport S., 2003, ApJ, 598, 431
Podsiadlowski P., Rappaport S., Pfahl E.D., 2002, ApJ, 565, 1107
Ritter H., 1988, A&A, 202, 93
Rohrmann R.D., Serenelli A.M., Althaus L.G., Benvenuto O.G., 2002, MNRAS, 335, 499
Sarna M.J., Ergma E., Gerškevitš-Antipova J., 2000, MNRAS, 316, 84
Schönberner D., Driebe T., Blöcker T., 2000, A&A, 356, 929
Serenelli A.M., Althaus L.G., Rohrmann R.D., Benvenuto O.G., 2001, MNRAS, 325, 607
Serenelli A.M., Althaus L.G., Rohrmann R.D., Benvenuto O.G., 2002, MNRAS, 337, 1091
Sigurdsson S., Richer H.B., Hansen B.M., Stairs I.H., Thorsett S.E., 2003, Sci, 301, 193
van Kerkwijk M.H., Bell J.F., Kaspi V.M., Kulkarni S.R., 2000, ApJ, 530, L37

This paper has been typeset from a TEX/LATEX file prepared by the author.